frontiers in Marine Science

ORIGINAL RESEARCH
published: 07 May 2019
doi: 10.3389/fmars.2019.00224

Sandbar Breaches Control of the Biogeochemistry of a Micro-Estuary

Yair Suari[1], Tal Amit[1], Merav Gilboa[1], Tal Sade[1], Michael D. Krom[2,3], Sarig Gafny[1], Tom Topaz[4] and Gitai Yahel[1]*

[1] School of Marine Sciences, Ruppin Academic Center, Michmoret, Israel, [2] Morris Kahn Marine Research Station, Department of Marine Biology, Charney School of Marine Sciences, University of Haifa, Haifa, Israel, [3] School of Earth and Environment, Faculty of Environment, University of Leeds, Leeds, United Kingdom, [4] Department of Soil and Water Sciences, The Robert H Smith Faculty of Agriculture, Food and Environment, The Hebrew University of Jerusalem, Rehovot, Israel

Micro-estuaries in semi-arid areas, despite their small size (shallow depth of a few meters, length of a few kilometers, and a surface area of less than 1 km^2) are important providers of ecosystem services. Despite their high abundance, tendency to suffer from eutrophication and vulnerability to other anthropogenic impacts, such systems are among the least studied water bodies in the world. In low tidal amplitude regions, micro-estuaries often have limited rate of sea-river water exchange, somewhat similar to fjord circulation, caused by a shallow sandbar forming at the coastline. The long-term study, we report here was inspired by the idea that, due to their small size and low discharges regime, relatively small interventions can have large effects on micro-estuaries. We used a stationary array of sensors and detailed monthly water sampling to characterize the Alexander estuary, a typical micro-estuary in the S.E. Mediterranean, and to identify the main stress factors in this aquatic ecosystem. The Alexander micro-estuary is stratified throughout the year with median bottom salinity of 18 PSU. Prolonged periods of hypoxia were identified as the main stress factor. Those were alleviated by breaching of the sandbar at the estuary mouth by sea-waves or stormwater runoff events (mostly during winter) that flush the anoxic bottom water. Analysis of naturally occurring sandbar breaches, and an artificial breach experiment indicate that the current oxygen consumption rate of the Alexander micro-estuary is too high to consider sandbar breaches as a remedy for the anoxia. Nevertheless, it demonstrates and provides the tools to assess the feasibility of small-scale interventions to control micro-estuaries hydrology and biogeochemistry.

Keywords: eutrophication, anthropogenic pollution, coastal stream, Mediterranean, sandbar, sill, estuaries

OPEN ACCESS

Edited by:
Isabel Iglesias, Interdisciplinary Center for Marine and Environmental Research (CIIMAR), Portugal

Reviewed by:
Perran Cook, Monash University, Australia
José Pinho, University of Minho, Portugal

****Correspondence:***
Yair Suari
yairsuari@gmail.com

Specialty section:
This article was submitted to Coastal Ocean Processes, a section of the journal Frontiers in Marine Science

Received: *22 November 2018*
Accepted: *10 April 2019*
Published: *07 May 2019*

Citation:
Suari Y, Amit T, Gilboa M, Sade T, Krom MD, Gafny S, Topaz T and Yahel G (2019) Sandbar Breaches Control of the Biogeochemistry of a Micro-Estuary. Front. Mar. Sci. 6:224. doi: 10.3389/fmars.2019.00224

INTRODUCTION

Estuaries, the enclosed water bodies where fresh water is mixed with sea water (Elliott and McLusky, 2002; Tagliapietra et al., 2009; Day et al., 2013), are aquatic ecosystems which are among the most dynamic, diverse, and productive in the world, and as such they are also highly sensitive to environmental disturbances (Barrett, 2002; Ducrotoy and Elliott, 2006). The sheltered waters of

healthy estuaries are home to rich and diverse communities where marine, aquatic, and terrestrial flora and fauna mix and interact. This diversity of ecological niches exists partly because of the high salinity and nutrient gradients created from the mixing of fresh stream water with seawater (Bárcena et al., 2012). Estuaries benefit mankind in a variety of ways, playing a vital role in the health of coastal communities (OJEC, 2000; Bárcena et al., 2012). For example, estuaries often serve as focal point for outdoor recreational activities, as nurseries for marine fish (Blaber et al., 2000) and as chemical reactors that absorb and remove nutrients, pollutants, and other chemical compounds (Sanders et al., 1997).

Estuary dynamics are controlled by an interplay between the river (discharge and water quality), sea (tides, waves, and currents), and the atmosphere (winds and rain), as well as by the local geomorphology (Sierra et al., 2002; Bianchi, 2007). In low tidal range and in arid regions many of the estuarine systems are intermittently and or partly closed due the formation of a sandbar (sometimes refers to as sill or berm) between the marine environment and the fresh water body (Gale et al., 2006; Hastie and Smith, 2006; Everett, 2007). Occasional breach of the sandbar can cause an increased river-marine water exchange that is commonly followed by rapid change of water quality (Barton and Sherwood, 2004; Gale et al., 2006; Schallenberg et al., 2010) and ecological assemblages (Hastie and Smith, 2006; Avnaim-Katav et al., 2016).

Due to the low rate of bottom water exchange, intermittently closed estuaries and lagoons or 'blind' estuaries have also been identified as prone to anoxic conditions (Gale et al., 2006; Schallenberg et al., 2010). This tendency to anoxic conditions is amplified by anthropogenic eutrophication resulting from urban, agricultural, and industrial wastes discharged, as well as by changes in land use (Rabalais et al., 2010) and dramatic reduction in natural freshwater flow. In some cases (Barton and Sherwood, 2004; Becker et al., 2009), artificial sandbar breaches were proposed and used to mitigate this problem, to increase the sea-river water exchange rate and increase estuaries performance as hatcheries. However, the duration and effectivity of such mitigation action have not yet been fully studied.

Micro-estuaries, identified as such by a depth of few meters, a length of a few kilometers and a surface area of less than 1 km^2, are among the least studied water bodies despite their abundance, especially in arid or semiarid regions such as Australia, California, and the Middle-East. It is also very likely that due to their small size, these water-bodies are among the most affected by anthropogenic activities. For instance, all 11 streams along the <200 km of Israel's Mediterranean coastal plain (**Figure 1b**) meet the above criteria with estuarine surface area of up to 0.5 km^2 and annual discharge $<20 \times 10^6$ m^3. All are also under severe anthropogenic pressures, first and foremost from sewage discharge, but also from anthropogenic utilization of water, damming, pesticide laden agricultural runoff (Topaz et al., 2018), and other man-made disturbances. Nevertheless, even at their deteriorated state, these micro-estuaries and coastal streams serve as biodiversity hotspots, critical nurseries for marine species, and focal points for vast recreation activity.

The Alexander micro-estuary is located in a semiarid region with a classical Mediterranean climate where anthropogenic factors have become more dominant as human population grows and land use practices become more intensive. Like many micro-estuaries (and many larger estuaries) in the region and elsewhere, most of the natural freshwater sources in its catchment area have been captured for human use and the residual flow is currently dominated by treated wastewater which makes the system hypereutrophied (Suari et al., 2017). Similarly hypereutrophied estuaries with more than 20 $\mu mol\ L^{-1}$ phosphate and or 300 $\mu mol\ L^{-1}$ nitrate have been found in all of the main Israeli coastal streams (Herut et al., 2015), in Lebanon (Baydoun et al., 2016), California (Kennison Krista Kamer and Fong, 2003; Kennison and Fong, 2014), and Spain (Velasco et al., 2006). The combination of arid conditions and increased anthropogenic water demand is likely to lead to the spreading of estuarine hypereutrophication (Kennison and Fong, 2014). Anecdotal observations suggest that micro-estuaries also exist in many other countries but hard data regarding the status of those systems is hard to obtain, likely due to the lack of awareness and resources for monitoring programs.

At the Alexander micro-estuary mouth, a sandbar is commonly formed under the combined effect of river flow and sea waves. The sandbar limits water exchange between the estuary and the open sea (Lichter et al., 2010). Sandbars at the mouth of estuaries in semi-arid climate zones have been described, but rarely thoroughly studied, in Australia, South America, and South Africa (Barton and Sherwood, 2004; Gale et al., 2006). Observations and anecdotal evidence suggests that the high abundance of such sandbars along the Mediterranean climate region coasts is reflected in other coastal regions where small streams reach the sea.

This study was inspired by the idea, originally proposed by Pye and Blott (2014) for "small estuaries," which are 50-fold larger than micro-estuaries, that due to their small size, relatively small interventions can potentially make large effects on function and health. Our goal was to thoroughly characterize a typical Mediterranean micro-estuary in terms of its bathymetry, hydrology, and biogeochemistry and to highlight the major stress factors in the system. Our preliminary data suggested that prevailing anoxic conditions, sustained by the heavy N and P loads resulting from poorly treated urban sewage discharged into the system, was the major stress factor. Therefore, we analyzed a series of natural sandbar breach events in order to study their effect on the oxygen status of the system, the underlying mechanisms that lead to these events, and the potential of artificial sandbar breach to serve as a mitigation measure to the anoxic conditions. The research is part of a multidisciplinary biological, ecological, physical, and managerial project that is intended to promote science-based rehabilitation strategies for Israel's micro-estuaries.

STUDY SITE

The Alexander stream flows through the Sharon coastal plain of Israel located between the Samaria mountains and the

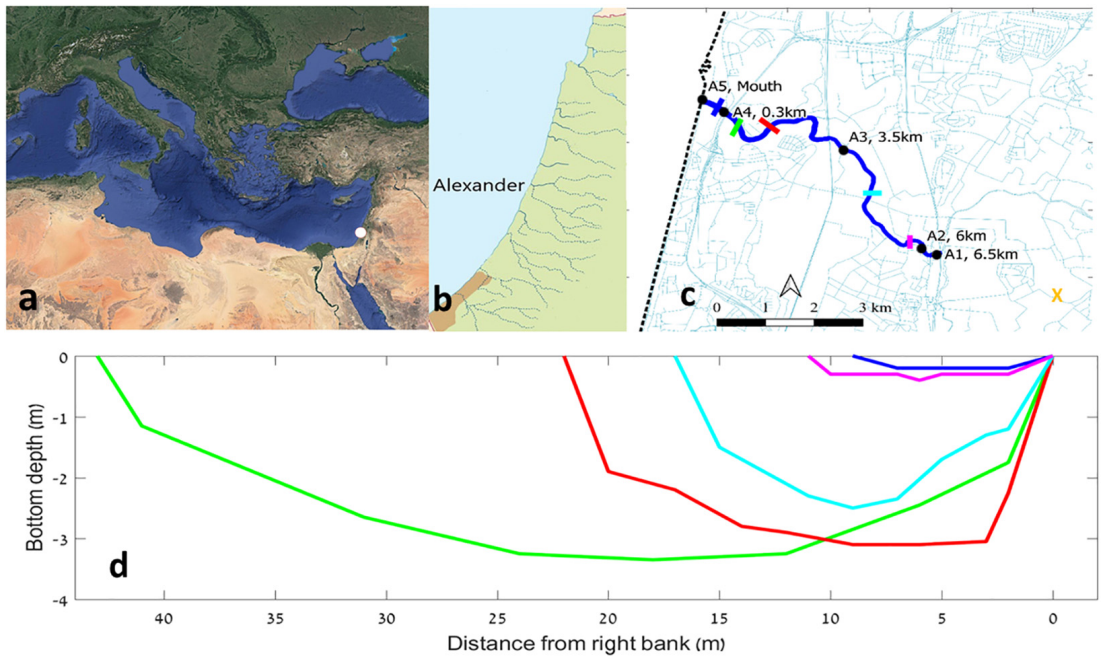

FIGURE 1 | The location of the Alexander estuary and its bathymetry. **(a)** The location of the estuary at the Mediterranean Levantine basin denoted by white dot. **(b)** Coastal streams along the Israeli coast. **(c)** A map of the estuary (in blue) and the location of the sampling points (black dots), bathymetry sampling cross sections (colored lines), and water inflow sampling station (orange "X" symbol). **(d)** Depth of bathymetric cross sections along the estuary. Each of the five series represent median bottom depth for a 300 m long section.

Mediterranean coast (**Figure 1**). It is ∼35 km long, draining a watershed of 560 km^2. The micro-estuary part of the Alexander, defined as the region where the river channel bottom is deeper than maximum sea level, extends ∼6.5 km beginning at an artificial weir. The Israeli coastline is affected by longshore drift which transports sand from the Nile delta to the south, northward as far Haifa bay. At the estuary mouth of the Alexander, there is a sandbar (sometimes composed of sand and gravel) which controls the flow of the Alexander stream to the sea (Lichter et al., 2010).

Historically, Alexander stream discharged freshwater to the sea throughout the year. During the dry season, approximately 8 months of the year, it drew water from aquifer springs, and supported a diverse ecosystem. However, currently, like in many other Mediterranean streams (Ludwig et al., 2009), there is almost no natural flow in the Alexander because the freshwater is used for human consumption. Present day flow is mostly insufficiently treated and untreated waste waters (Herut et al., 2000, 2015; Ozer et al., 2015).

While the water quality in many of Israel's coastal streams has improved significantly in the last decades, for the Alexander this trend has stopped, and water quality has deteriorated since the early 2000s (Herut et al., 2015) when urban effluents started to flow into the Alexander tributaries (Tal et al., 2010). At the time of writing, a new waste water treatment plant is being constructed which is expected to divert the effluents for agricultural use by 2022 so that no wastewater or treated water will be discharged into the estuary.

At the marine side of the Alexander estuary, the south east Levantine basin of the eastern Mediterranean, is an evaporative basin characterized by temperatures ranging from ∼15 to ∼30°C and salinities ranging from ∼38.6 to 40 PSU (Hecht et al., 1988; Ozer et al., 2015). The basin is ultra-oligotrophic, and the surface water maximal inorganic nutrient concentration rarely exceeds 0.05 and 3 μmol L^{-1} for phosphate and nitrate, respectively (Azov, 1991; Krom et al., 2005; Krom and Suari, 2015).

The Mediterranean climate is characterized by a winter rainy season from November to April (Goldreich, 2003). Most of the rain during the rainy season is concentrated in ∼10 rain events (Saaroni et al., 2010). A typical rain event is caused by a low-pressure system approaching the eastern Mediterranean from Europe. Along the Israeli coast, these events often begin by an intense (usually 15 m s^{-1}) southern wind gradually rotating to the west while intensifying and eventually reaching a north westerly direction and declining (Goldreich, 2003; Saaroni et al., 2010). The wind is accompanied by a rapid increase of wave height several hours after the beginning of the southern wind and by rain storms, usually when the wind reaches a westerly direction. These rain storms can occasionally lead to stormwater floods in the Alexander and other coastal streams.

The Mediterranean is defined as a microtidal basin and the astronomic tidal range along the Israeli coastline has an amplitude lower than 0.4 m in 93% of the tides (Striem, 2015). Therefore, most of the sea level variations are attributed to wind surge (Rosen, 2000; Striem, 2015). A recent study (Shalem et al., 2014) has shown that both storm surge and stormwater runoff

events can cause elevated bottom salinities at the Alexander estuary and that it is, therefore, more stratified during winter.

MATERIALS AND METHODS

The study took place between January 2014 and June 2016, in the mid Mediterranean coastal plain of Israel, Alexander estuary (**Figure 1**). All data and protocols are available at the RECO (Ruppin Estuarine and Coastal Observatory)[1].

Bathymetric Survey

Bottom depth measurements were conducted by towing a bottom looking sonar integrated with GPS (Humminbird 385Ci) behind a kayak. The kayak scanned the estuary in an S shaped course with a mean distance of ∼20 m between loops. The estuary surface level was aligned to mean sea level once every 2 h by comparing estuary surface water to a reference point measurement using a differential GPS (Topcon GR3).

Continuous Measurements

Freshwater influx into the estuary was measured by the Israeli Water Authority using a hydrograph with a calibrated water level buoy, located ∼500 m upstream of the estuary head (**Figure 1c**) with hourly resolution during winter stormwater runoff events and twice daily during baseflows.

A stationary array of moored sensors was used to measure Water level (Hobo/OnSet), temperature and salinity (DST CT salinity and temperature logger, Star Oddi) and dissolved oxygen concentration (U26-001, HOBO, Onset/RBR SoloDO). The array consisted of two sets of sensors, one for surface water and one for deep (near bottom) water and was deployed ∼350 m upstream from the estuary mouth (**Figure 1c**). The bottom water sensors were connected to a cable and kept near the bottom by a lead weight. The surface sensors were connected to a float that kept them ∼20 cm below the surface. The cable carrying the sensors was inserted into a metal tube mesh to protect it from fouling, vandalism and objects carried by the flow. All sensors were programmed for 5-min measurement intervals and were serviced and calibrated monthly. Retrieval/deployment cycle took few hours, and then the sensors were returned to the exact same position. After quality checks, all data has been uploaded to the research website where it is freely available to the public.

Monthly Sampling

Water Sampling was conducted monthly in five stations along the estuary during the last week of the month, from January 2014 to June 2016 (total of 30 sampling sessions). Station locations are depicted in **Figure 1**. Both physical and chemical parameters were measured in each station. Vertical profiles of temperature, salinity, and oxygen concentration were measured using a SeaBird, SBE19Plus V2 CTD equipped with a dissolved oxygen sensor (SBE43, Seabird) chlorophyll fluorometer (Cyclops 7, Turner Design) and an optical backscatter sensor (OBS3+, Campbell Scientific). Discrete water samples were taken in each station, using horizontal water sampler (5L, Model 110B, OceanTest Equipment). Where and when water depth exceeded 0.5 m, samples were taken from surface water (∼20 cm below surface) and deep water (∼20 cm above bottom) otherwise, only surface water were sampled.

Water samples for inorganic nutrients (nitrate, nitrite, ammonium, and phosphate) were drawn directly from the Niskin spigot into a disposable syringe and filtered at the field through a 0.2 μm syringe filter (32 mm, PALL Acrodisc). Samples for biological oxygen demand (BOD), total and organic suspended matter and chlorophyll *a* were collected into dark bottles. All samples were kept in a cool box on ice. Upon arrival to the laboratory (up to 4 h), 10 mL of the water was filtered onto glass fibers filters (25 mm, Whatman GF/F) for chlorophyll *a* analysis. Similarly, samples for total suspended solids (TSS) and particulate organic matter (POM) were filtered (normally 100–200 mL) on 47 mm GF/F filters (Whatman). Filters and nutrient samples were kept frozen in −20°C until further analysis.

Samples for BOD_5 were aerated to saturation (at least 1 h), diluted to 1:5 ratio with air saturated double distilled water, transferred into 330 mL BOD bottles and analyzed using a YSI 5100 (YSI) according to the standard method (Celesri et al., 2012).

Chemical Analysis

Nutrients determination was carried out manually following standard methods (Grasshoff et al., 2009). Briefly, water for nitrite and nitrate determination was diluted ×100 with double distilled water prior to analysis. Nitrate and nitrite were determined after reduction to nitrite on a cadmium–copper column by combination with a diazo-dye and measured spectrophotometrically (Morris and Riley, 1963). The ultimate precision was calculated at ±8% (14 μmol L^{-1}) for nitrate and ±10% (2.5 μmol L^{-1}) for nitrite based on the variability of triplicates taken in each sampling session.

Phosphate concentration was also measured spectrophotometrically following the Murphy and Riley (1962) molybdate blue method after ×10 dilution with double distilled water. The precision was similarly estimated as ±4% (1.5 μmol L^{-1}).

Ammonium concentration was determined using a modified version of the Holmes et al. (1999) protocol as described in Supplement 1 of Meeder et al. (2012) after ×1000 dilution with double distilled water. Briefly, the method uses ortho-phthalaldehyde (OPA) that forms a fluorescent complex with ammonium. To account for the variability of the estuarine water that results from the highly variable matrix effect, an internal calibration curve was produced for each water sample by spiking three of the four 2 mL aliquots drawn from each water sample being analyzed, with known concentrations of ammonium standard solution. After the samples were spiked, 0.5 mL of OPA solution was added to each aliquot, the samples were then incubated at room temperature in the dark for 3–4 h. Fluorescence of the OPA-ammonium complex was read using the ammonium channel of an Aquafluor fluorometer (Turner Designs). Corrections for background fluorescence were determined by measuring the fluorescence of additional aliquot

[1] http://reco.ruppin.ac.il/eng/

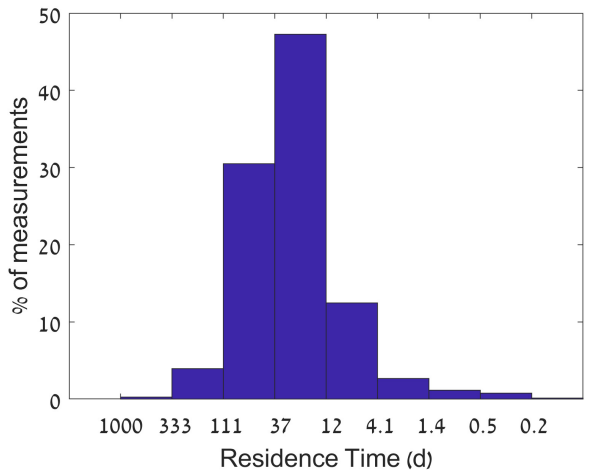

FIGURE 2 | Histogram of estimated residence times from January 2014 to August 2016. Residence times (*X*-axis) are calculated from influx measurements assuming a constant estuary volume of 300,000 m^3. The *Y*-axis represents the percentage of occurrences.

immediately after the addition of OPA. The precision is estimated as ±4% (14 μmol L^{-1}).

Chlorophyll *a* concentration was determined using the modified dimethyl sulfoxide (DMSO) extraction method of Burnison (1980), with small modifications. Briefly, after sample filtration, the glass fiber filters were placed in vials with Teflon lined screw caps. Two milliliters of DMSO (reagent grade) was added and the vials were incubated at 65°C in dark for 30 min. Then, vials were cooled to room temperature, and 4 mL of buffered aqueous Acetone (90% acetone, 10% saturated $MgCO_3$ solution) was added to the vials. The vials were vortexed roughly and left in order for the solid suspension to sink. Fluorometric readings were taken using a Trilogy fluorometer (Turner designs).

Sandbar Breach Experiment

A field sandbar breach experiment was conducted to test the effect on the water column properties under controlled conditions. The breach was initiated on March 9, 2015 at 16:30 using a Caterpillar shovel that created a channel between the sea and estuary. The sea and estuary channel remained connected for less than 10 h and by the morning the sandbar had reformed.

Data Analysis

Bathymetric data analysis was conducted using QGIS (QGIS Developement Team, 2017) and Matlab (MathWorks Inc, 2012). Due to the long and narrow structure of the estuary, longitudinal differences in depth were milder than the difference across the estuary, causing disturbances when linearly interpolating the measured data. Therefore, the rectangular coordinate system was transformed to flow oriented coordinate system (Merwade et al., 2008) in which *X* and *Y* were represented as *L* (length along flow line from estuary mouth) and *W* (distance from right bank). *L* values were divided by 100 to achieve an *L*/*W* ratio adequate for linear interpolation. The depths were then linearly interpolated using Matlab and re-projected to the rectangular coordinate system.

To identify biogeochemical processes that were not related to the dilution of eutrophic stream water with the nutrients and chlorophyll deprived Mediterranean water, the nutrients and chlorophyll *a* concentration were linearly normalized to salinity (assuming constant seawater salinity of 39.5) as presented in Eq. (1).

$$C_{norm} = C_a \frac{39.5}{S_a} \quad (1)$$

Where, C_{norm} is the normalized concentration, C_a is the ambient (measured) concentration, and S_a is the ambient (measured) salinity.

Water depth of the estuary varied with time. To simplify the data representation, all bottom samples (deeper than 0.5 m) were plotted at 0.3 m above the bottom during the deepest encountered sampling day. The normalized concentrations were plotted in three dimensional plots using ODV (Schlitzer, 2018) using weighted average gridding method.

The sensors data analysis was conducted using Matlab (MathWorks Inc, 2013). Identification of prominent mixing events was conducted by first calculating a time series of daily salinity median for the bottom sensor and then calculating a dilution percentage with either seawater when salinity increased [Eq. (2), $S_2 > S_1$] or freshwater [Eq. (3), $S_2 < S_1$] when salinity decreased for that time series.

$$\frac{S_2 - S_1}{39.5} \quad (2)$$

$$\frac{S_2 - S_1}{S_1} \quad (3)$$

Where, S_2 is the later day median salinity and S_1 is the first day median salinity. 39.5 is the typical seawater salinity in the study site.

Wave height and rain during maximum and minimum salinity changes (sandbar breaches) were extracted from the IOLR global sea level observing system (Tolkatchev, 1996) at Hadera port[2], ∼8 km from the estuary mouth.

The effect of sea-estuary water exchange on water column oxygenation was evaluated by sorting the day to day salinity changes from lower values (stormwater runoff events) to the highest value (seawater entrance to bottom water) and matching the daily oxygen concentration derivative for each salinity derivative.

RESULTS

Bathymetry

The Alexander estuary stretches 6.5 km long from a constructed dam with an artificial waterfall at the shallow (0.2–1.2 m) and narrow (4–10 m) estuary head at the east (**Figure 1c**). Downstream from the head, the estuary gradually deepens and

[2]http://isramar.ocean.org.il/isramar2009/Hadera/

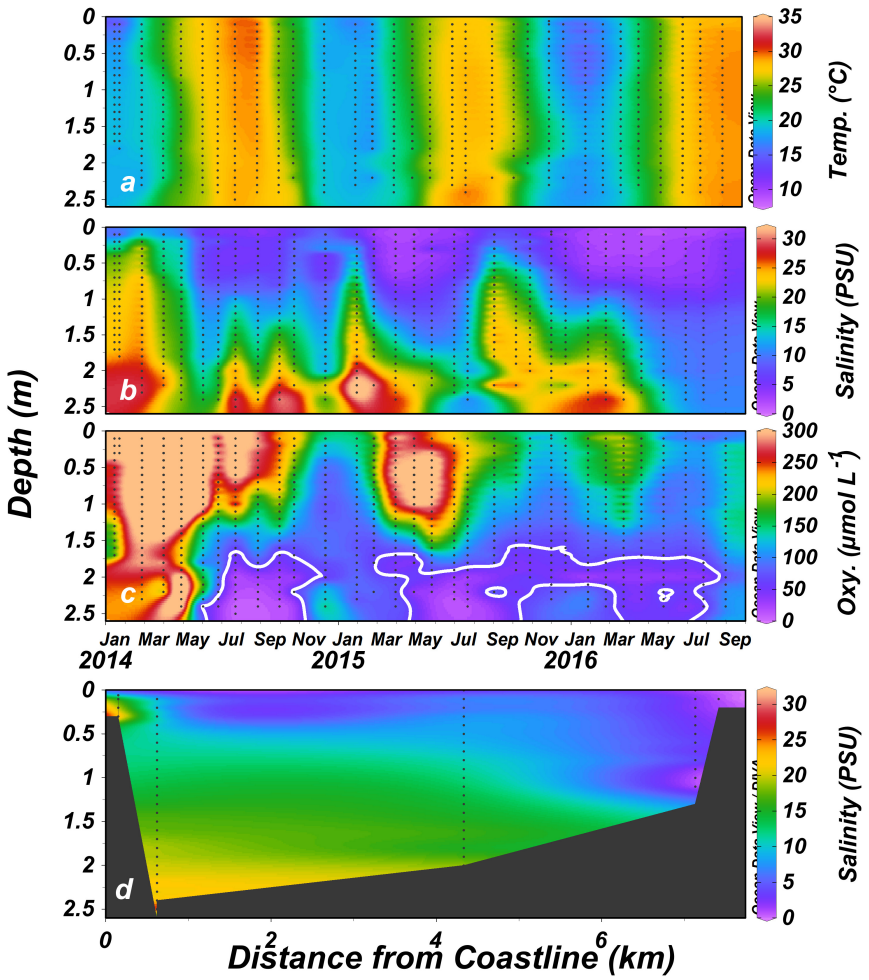

FIGURE 3 | Temperature **(a)**, salinity (PSU) **(b,d)**, and dissolved oxygen (µmol L^{-1}) **(c)** ∼350 m upstream from the Alexander estuary mouth (January 2014 to August 2016). The white contour lines in **(c)** represent hypoxic conditions. Black dots represent sampling locations. The average salinity distribution throughout the research period is presented in **(d)**.

widens until it reaches the deepest and widest point (∼45 m wide and ∼3 m deep), ∼300 m upstream from the estuary mouth. Based on the bathymetric structure and the typical estuary water elevation, the volume of the estuary under baseflow conditions was calculated to be ∼300,000 ± 100,000 m^3.

The estuary mouth is usually less than 10 m wide and 0.5 m deep. However, its structure can be dynamic as dictated by sea and fresh water currents and waves (Lichter et al., 2010). Usually, the estuary morphology is constant during summer (aside from water level fluctuations of up to 1 m, see below) but during winter, stormwater runoff events can cause significant bathymetric changes.

The estuary surface water elevation ranged −0.5 m to 1.5 m above sea level (**Supplementary Figure S1**). With a median elevation of 0.29 m during summer and 0.19 m during winter. Our observations suggest that the main controllers of surface water elevation were sandbar morphology combined with fresh water entry (stormwater runoff events), and or sea surface elevation (waves and surge).

Freshwater Influx

Under baseflow conditions, water flux to the estuary is controlled by the discharge of effluents from the sewage treatment plant at Yad Hanna, 12 km upstream from the estuary head, that provides a stable influx (median 11.5 × 10^3 m^3 day^{-1}) resulting in long residence times of ∼25 days. The residence time was drastically reduced to less than 1 day during winter stormwater runoff events, which occur ∼2% of the time (**Figure 2**). Damming and pumping of stream water for irrigation during winter actually reduced the base flows. We define stormwater flow events as discharge larger than 10^5 m^3 day^{-1}. Such flows occurred for less than 2 weeks a year.

Hydrology

The physical properties of the water column are almost solely controlled by the water salinity and the effect of temperature on water density and water column stability was usually negligible (data not shown). The salinity profile was usually stratified,

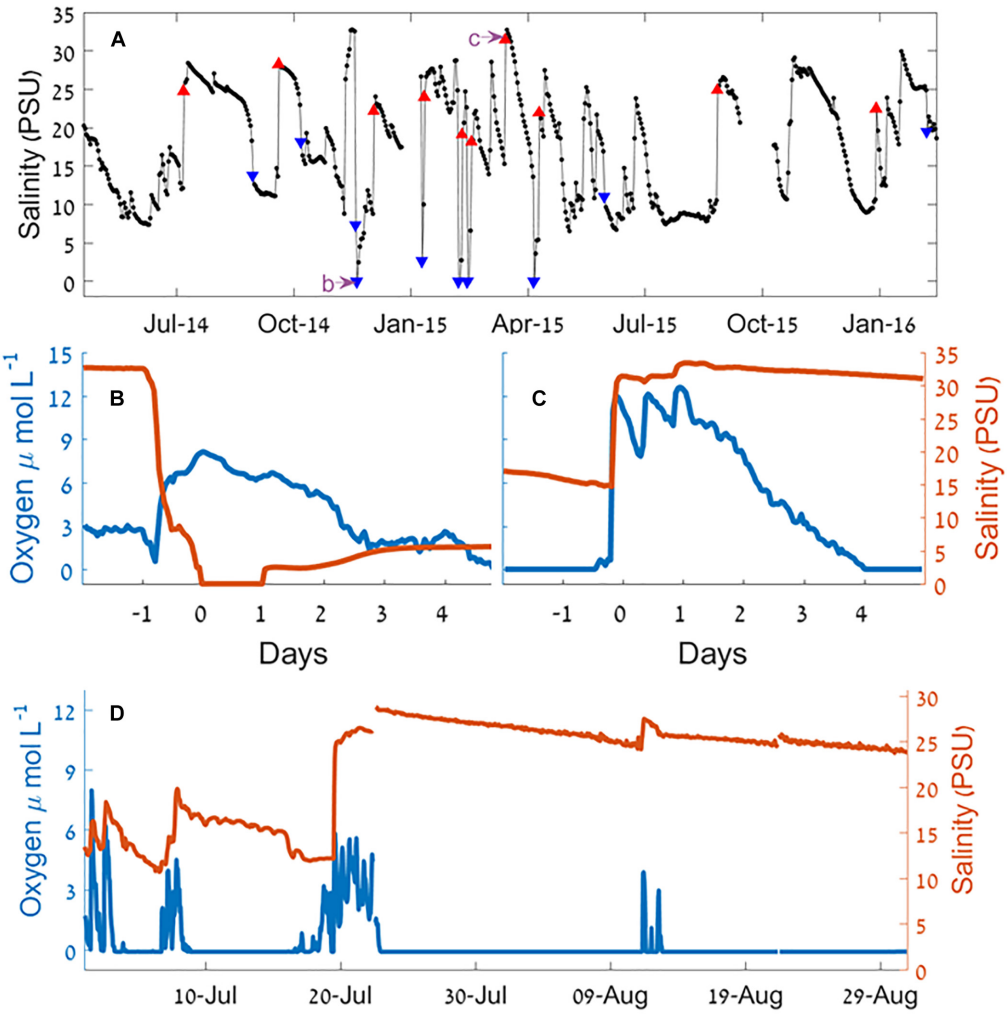

FIGURE 4 | Salinity and oxygen at the Alexander estuary bottom water 350 m upstream from the estuary mouth during a sandbar breach. **(A)** Time series of daily medians of salinity January 2014 to August 2016. The blue triangles represent the 10 largest salinity decrease events and the red triangles represent the 10 largest salinity increase events. The purple arrows point the timing of panels **(B,C)**. **(B,C)** A 6-day time series of sandbar breach causing salinity decrease **(B)** and increase **(C)** and the effect on oxygen concentration. **(D)** A time series of salinity and oxygen concentration during the summer of 2014. For a detailed view of the marked events, see **Supplementary Figures S4**, **S5**.

with saline bottom water (average of 28 PSU, ∼70% seawater) overlaid by the fresher water (ranging from <1 PSU at the head to over 5 PSU near the mouth) originating from the estuary head (**Figure 3a**). The halocline was commonly located at ∼1 m depth. Stratification was gradually dissipated upstream and at the estuary head sea-born salinity was rarely found.

Continuous recording using moored sensors ∼350 m from the estuary mouth (**Figure 1c**) revealed fluctuations of bottom water salinity (**Figure 4** and see also **Supplementary Figures S3**, **S4**). These temporal gradients were mostly gradual but could be steep, sometimes changing from 33 to 0 PSU (87–0% seawater) over a period of few hours. Typically, the positive salinity shifts (seawater entrance) showed steeper gradient whereas negative shifts (removal of salt) were more gradual (with the exception of flood events). During most winters, the estuary salinity was higher and more variable.

Since events involving changes of salinity that were much higher than the typical day to day changes were caused by breaching of the sandbar, our analysis of the effect of breaches began by analyzing the 20 sharpest salinity gradients (10 largest increase and 10 largest decrease events, **Table 1**), of these, 16 occurred during the winter rainy period (November–April). Eight out of the 10 salinity decrease events were accompanied by heavy rain events, and six of them were accompanied by high seas (significant wave height >1.5 m). Of the salinity increase events, six were accompanied by heavy rains and four by high seas.

Geochemistry

The estuary was hypereutrophic throughout most of the study period due to high loads of organic matter, nitrogen, and phosphorus in the inflow from the head (dissolved inorganic nitrogen, DIN 870 ± 500 μmol L^{-1}, phosphate 45 ± 53 μmol

TABLE 1 | Mechanisms of sandbar breaches: 20 sandbar breaches identified by large day to day change of the bottom salinity 350 m upstream from estuary mouth.

Temporal derivative sign	*N*	Hs > 1.5 m	Heavy rain	Pre-storm
Negative (decreasing salinity)	10	6	8	
Positive (increasing salinity)	10	4	6	4

Hs, significant wave height; heavy rain, more than 20 mm rain during the 48 h before the breach; pre-storm, breaches that occurred within 24 h before a rain event.

L^{-1}, mean ± 1 SD, **Figure 5** and see also **Supplementary Figure S2**). These values tended to diminish toward the estuary mouth (39% and 22%, respectively). Phytoplankton blooms dominated the estuary surface water, with chlorophyll values increasing downstream ∼75% from an average of 101 ± 94 μg L^{-1} at the head to 177 ± 117 μg L^{-1} at the mouth, mirroring the trend observed for inorganic nutrients. Ammonium, accounted for most of the DIN under the anoxic conditions that prevailed at the bottom water, especially in the stagnant waters that typified the mid-estuary region. By contrast, nitrate dominated the more oxygenated surface water (**Figure 5a**).

Dissolved oxygen concentrations were on average higher at the surface and downstream toward the mouth. The stagnant bottom water at the mid estuary, ∼3 km from the estuary mouth (**Figure 1c**) was anoxic (<3 μmol L^{-1} dissolved oxygen, Celesri et al., 2012) during all monthly sampling campaigns. Continuous measurements of dissolved oxygen concentration showed strong daily fluctuation at the surface water, ranging from 0 to >200% saturation. Overall, hypoxic (<63μmol L^{-1}, Madden et al., 2009) and anoxic condition prevailed in the surface water during 11% and 48% of the time, respectively. Anoxic concentration also characterized the deeper water at the sampling station located ∼350 m upstream from the estuary mouth, where anoxic and hypoxic conditions prevailed during 68% and 9% of the time, respectively. BOD (**Supplementary Figure S5**) was very high with a minimum, median and maximum of 73, 445, and 1,509 μmol L^{-1} d^{-1}, respectively.

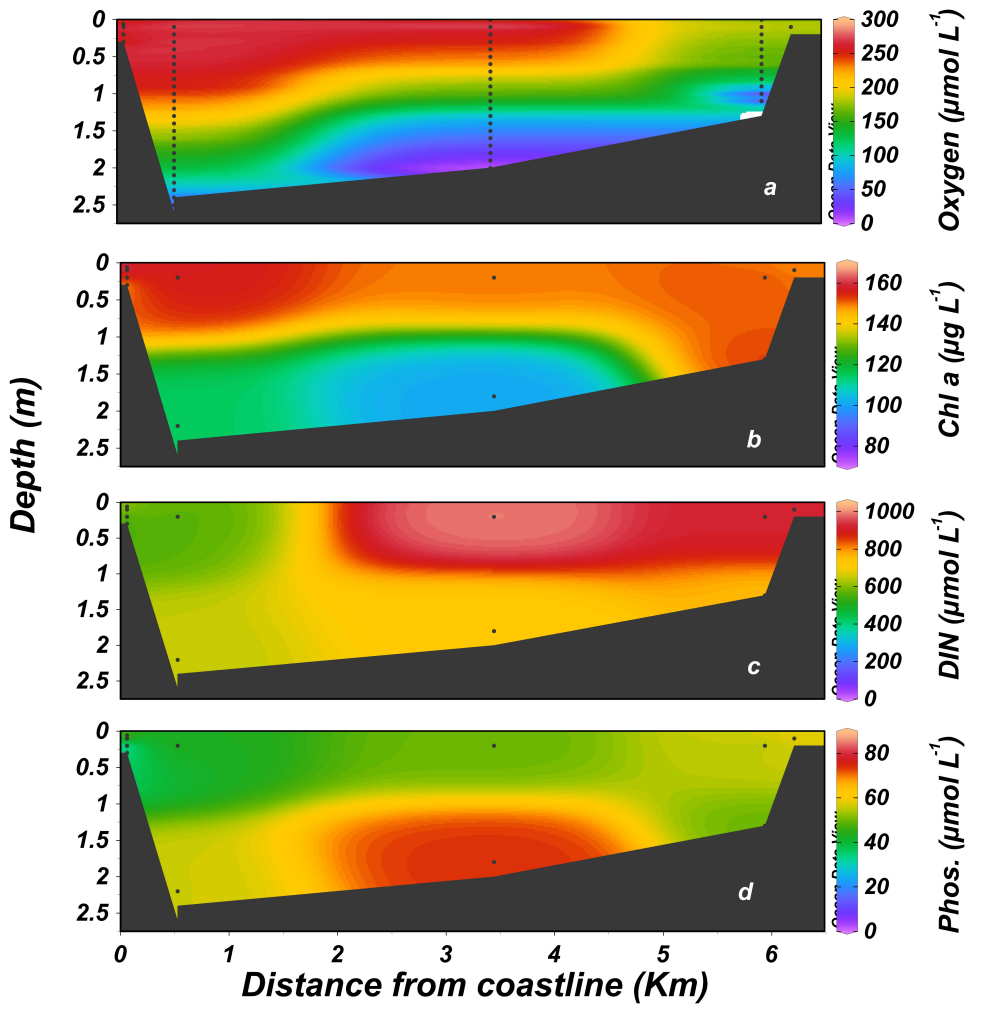

FIGURE 5 | Distribution of dissolved nutrients, dissolved oxygen and chlorophyll *a* along the Alexander estuary. January 2014 to August 2016. **(a)** Dissolved oxygen, **(b)** chlorophyll *a*, **(c)** dissolved inorganic nitrogen (DIN, calculated as NO_3+NO_2+NH_4), **(d)** phosphate. Black dots represent sampling locations.

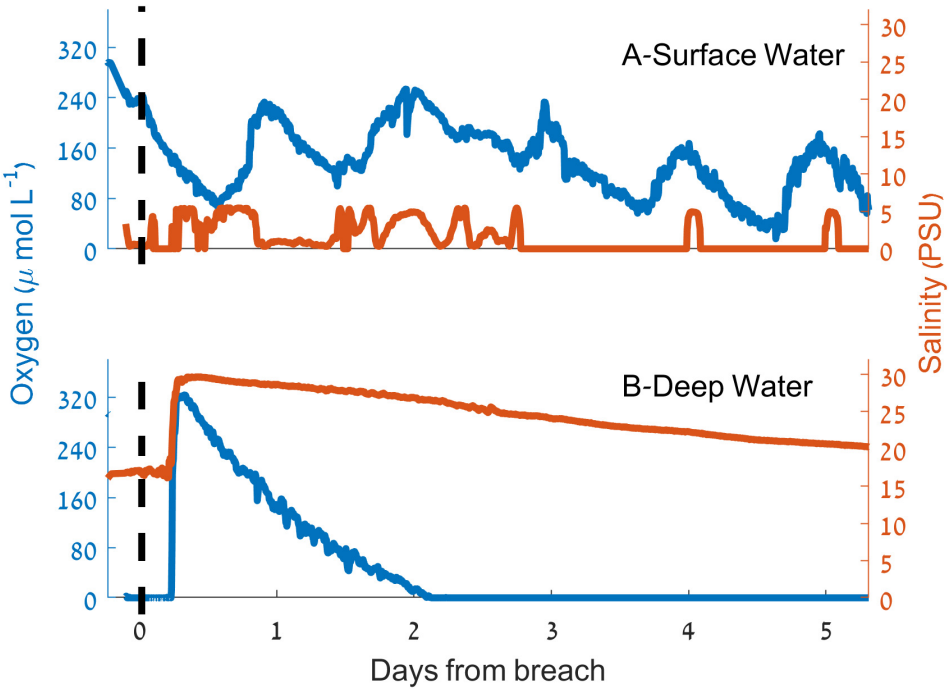

FIGURE 6 | Dynamics of salinity (red) and dissolved oxygen concentration (blue) during the sandbar breaching experiment. **(A)** Surface water. **(B)** Deep water. The vertical dashed lines indicate the time of the breach.

Sandbar Breaching Experiment

During the sandbar breach experiment (March 9–15, 2015) an increase of 13 PSU in the salinity of deep water samples ∼350 m upstream from the estuary mouth was observed within 3 h of the sandbar breach (**Figure 6**). This increase was accompanied by an increase of oxygen concentration from 0 to 324 μmol L^{-1} (>130% of saturation, ∼10.5 mg L^{-1}). Shortly after this sharp increase of salinity and oxygen concentration, both, salinity and oxygen began to decline to their initial concentrations. However, the rate of decline was not equal and while the salinity decrease was more gradual, the bottom water oxygen concentration returned to anoxia within 2.5 days of the breach (**Figure 6**). In contrast to the near bottom water, surface water oxygen concentration and salinity changed only marginally as a result of the sandbar breach (**Figure 6**) with a slight reduction in surface water oxygen and small increase in salinity. About 24 h after the breach, the surface oxygen concentration seems to be affected only by the diurnal cycle while the salinity reaches close to zero with sporadic increases to ∼5 PSU mostly during the afternoons.

Effect of Natural Sandbar Breaches

Although continuous monitoring of the sandbar status was not always possible, our observations suggest that both important influx events of seawater into the estuary (salinity increase at the bottom water), and efflux of the estuary water to the sea (salinity decrease) that caused sharp salinity gradients were always associated with a breach of the sandbar. When the bottom water is anoxic, as was often the case in the Alexander, both influx and efflux of water through the estuary mouth in magnitudes higher than the typical flux were associated with sharp increases of the dissolved oxygen concentration.

The day to day changes of salinity in the bottom water (**Figure 7** and **Supplementary Figure S6**) were generally moderate and typified with small addition of fresh water (median dilution of 1.5%). A daily dilution with more than 5% of fresh water occurred in 17.5% of the days, whereas a daily dilution with more than 5% of sea water occurred in only 7.5% of the days. Changes in dissolved oxygen concentration were also generally mild (median decrease of 6 μmol L^{-1}). A major increase of bottom oxygen was usually associated with large salinity changes in the bottom water of the estuary (stormwater runoff events, 25 of the 630 research days and seawater influx, 50 of the 630 research days). Only larger stormwater runoff events that were associated with a large decrease of bottom water salinity, and presumably replacement of bottom water, increased the dissolved oxygen concentration (by up to 250 μmol L^{-1}). In contrast, breaches associated with even minor seawater intrusion caused the dissolved oxygen to increase in direct proportion to the salinity change (**Figure 7**). This implies that the seawater was an important oxygen source to the bottom water during seawater flushing events.

DISCUSSION

The goal of the present study was to characterize the coastal section of the Alexander stream as an example of a typical partially connected eastern Mediterranean micro-estuary

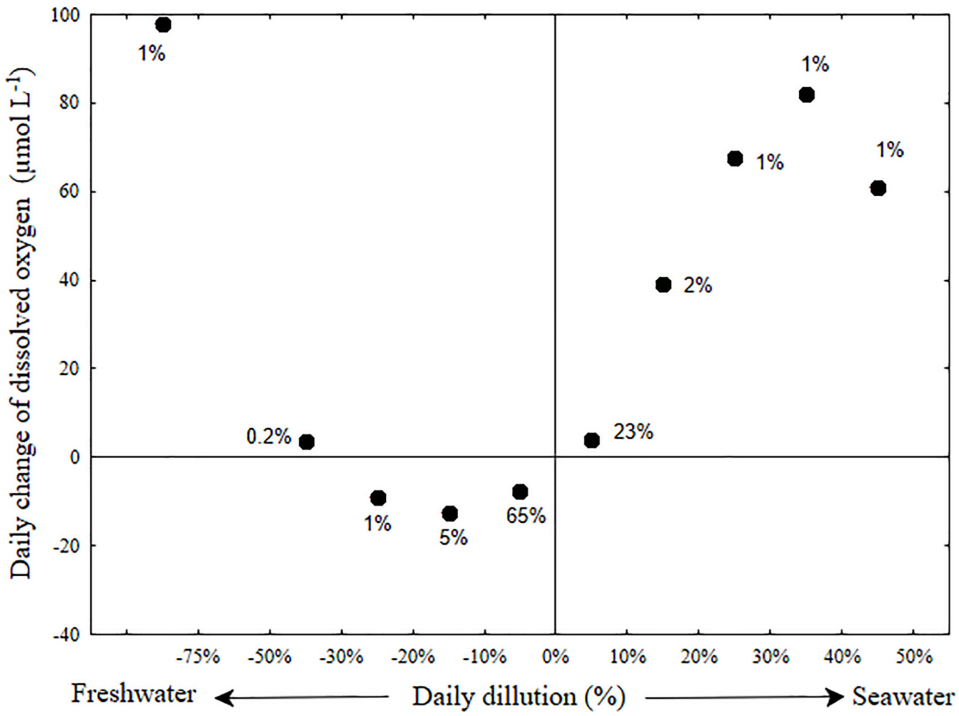

FIGURE 7 | Dilution oxygenation diagram of the Alexander estuary bottom water. The day to day oxygenation rate (*Y*-axis) averaged for each bin of daily dilution rate (*X*-axis). Error bars were removed for clarity (see **Supplementary Figure S6**). The term daily dilution refers to the percent of water replaced by seawater or freshwater calculated from the salinity change. Positive values refers to dilution with seawater and negative values to dilution with fresh water. Day to day oxygen change, refers to the difference between the median of oxygen concentration measured on consecutive day. The labels near the datum indicates the percentage of days (out of a total of 559 days) in each bin.

(surface area of ∼0.15 km^2, <3 m deep, 10–30 m wide, and 6.5 km long), to identify the key stressors for this ecosystem, and to assess the effect of sandbar breaches (natural and artificial) in controlling the estuarine geochemistry.

Micro-Estuarine Dynamic

Despite its small size and shallow depth, the hydrography of the coastal section of the Alexander exhibits typical estuarine circulation throughout the year. The fact that this minute water body maintains this well stratified hydrographic structure, is explained by the low freshwater inflow (baseflow is typically ∼600 m^3 h^{-1}, **Figure 2**) that results in slow current velocities, and the lack of a significant tidal effect (tidal range ∼0.4 m). The long and narrow meandering channel structure of the estuary (**Figure 1**) and the well-developed riparian vegetation, limit the wind fetch length and prevent the formation of significant waves within the estuary. This combination of low current velocities, lack of waves and low tidal range limits vertical mixing. Such long and narrow estuarine channels are typical to the Israeli micro-estuaries and their riverine appearance may explain why, until recent years, these ecosystems were referred to, and treated as, "coastal streams" and their estuarine nature was rarely acknowledged. The low mixing rates at the micro-estuary and low freshwater influx (typically <8% of the estuary volume per day) support strong stratification with typical salinity difference of >10 PSU between the fresh water layer above and the saline layer below. Vertical gradients are often dramatic, sometime reaching 20 PSU in 20 cm. However, while the vertical stratification can be maintained undisrupted for many weeks, the small size of the micro-estuary also facilitates dramatic temporal changes and stormwater runoff events, or sea waves can erase or build up to a 25 PSU vertical salinity gradients within hours.

Water column geochemistry was highly affected by the combination of strong vertical stratification and eutrophication. Surface water oxygen concentration often varies daily (particularly in summer) from oversaturation to anoxia while the bottom stagnant water is mostly anoxic with much reduced diel variability.

A distinct anoxic "dead-zone" is usually found at the central section of the micro-estuary where a stagnant water mass can be maintained for many weeks (**Figures 3**, **4**). As is typical of large-scale dead-zones, the anoxic conditions at the Alexander dead-zone were likely a consequence of the high loads of anthropogenic derived nutrients and organic matter entering the estuary. The high nutrient influx nourishes large phytoplankton populations that develop along the estuary evident by the strong diel cycle of dissolved oxygen concentrations and longitudinal increase in chlorophyll *a* concentration toward the estuary mouth (**Figure 5b**). Dense phytoplankton blooms causes a reduction in light penetration (median Secchi depth 0.3 m, see text footnote 1), limiting primary production through most of the estuary. The limited light availability in conjunction with vertical stratification

causes intensification of the anoxic conditions (Smith et al., 1999; Schindler, 2012). DIN and PO_4 show different behavior in this dead zone (**Figure 5** and see also **Supplementary Figure S2**). Phosphate accumulated likely due to the breakdown of labile organic matter and release of iron-bound particulate P in anoxic waters (Krom and Berner, 1981) while total DIN was reduced at the bottom, most likely due to denitrification (Seitzinger and Sanders, 1997; Boyes and Elliott, 2006), as the main DIN species switched from nitrate in surface waters to mainly dissolved ammonium in the dead zone. This pattern was maintained by the highly stratified nature of the estuary and deep water stagnation (Diaz and Rosenberg, 2008). Oxygen stress is probably intensified by the low currents that lead to low turbulence rate (Borsuk et al., 2001).

Marine dead zones (Diaz and Rosenberg, 2008) have been found in many regions of the world and are linked with estuarine systems and coastal waters. Our findings indicate that in micro-estuaries such as the Alexander, that are located in arid region and discharge into oligotrophic coastal waters (where nutrient fluxes are small and the marine system is too "nutrient starved" to form anoxic conditions) dead zones do appear, but they are confined to the river channel. This contrasts to areas such as the Gulf of Mexico or the Chinese coastal shelf where such discharges cause hypoxic zones on the coastal shelf (Rabouille et al., 2008).

Anoxia was identified as the main stress factor in the Alexander estuary (Suari et al., 2017) as in other partially connected estuaries (Gale et al., 2006). Events of high-water exchange between the sea and the estuary due to stormwater floods or seawater intrusion temporarily remedied the anoxia (**Figures 5**, **6**), but these usually maintained the bottom water oxygenation for only short periods. Reduction of the nutrient laden freshwater inflow, due to pumping for agricultural use during the drought of 2014, resulted in a prolonged oxygenated condition that lasted several weeks until the inflow was resumed as described by Suari et al. (2017). Similarly, the recent resumption of pumping during the water shortage of summer 2018 also resulted in oxygenation of the estuary for several weeks (Suari et al., unpublished). These observations suggest that simple managerial means that will reduce nutrient influx and elevate bottom water exchange rate are expected to achieve relatively long-lasting remediation of the bottom water anoxia.

Sandbar Breach Effects

The sandbar in partially closed estuaries can be breached naturally or artificially (Potter et al., 2010; Schallenberg et al., 2010), a process that increases the water exchange between the estuary and the sea. This has been suggested as a possible management tool to control anoxia in such estuaries (Barton and Sherwood, 2004). Using the continuous sensors measurements (**Figure 4**) and frequent visual observations of the estuary mouth and sandbar (**Table 1**), we examined and identified three natural mechanisms causing sandbar breaches in Alexander estuary which re-oxygenated the water in the estuary.

(1) *Flood induced breach*: Increased riverine inflow occurs when large stormwater runoff or events caused by major rainfall events in the catchment area inject large amounts of water into the estuary over a short period of time (more than the estuary volume per day). This type of breach was associated with initial rapid decrease of bottom salinity (e.g., **Figure 4B**) sometimes completely erasing the sandbar or deepening the sandbar at the estuary mouth to well below sea-level. In most of these freshwater flood events a second phase took place after the flood event, which was an elevation of the bottom salinity as seawater entered the estuary through the breached sandbar (**Figure 4B**).

(2) *Wave induced breach:* In the coastal area adjacent to the Alexander estuary the sea waves are primarily created by onshore winds, which can under some conditions lead to a surge of sea water level (Zviely et al., 2007). The effect of the sea level surges is to cause sea level to rise above the estuary surface water and the sandbar, leading to a breach in the sandbar across the mouth of the estuary and the intrusion of salty, denser and oxygenated seawater into the estuary. It should be noted that when the sandbar is fully developed, e.g., by the end of the summer, it can reach a width of over ∼50 m. Under such circumstances, wave breaches can rarely occur because waves and surge are not normally energetic enough to breach the sandbar.

(3) *Gradual estuary level rise breach:* When no energetic events such as floods and sea storms are present for a prolonged period of time (usually during summer) and the sandbar separation between the estuary and the sea is complete, the estuarine water level will rise gradually due to the influx of base-flow freshwater, sometimes causing estuarine surface to rise up to 1 m above the sea level. Under such circumstances, overflow above the sandbar gains considerable velocity and starts eroding the sandbar further causing more estuarine water to flow to the sea and eventually breach the sandbar completely. These gradual level rise breaches can reduce the estuary water level by about 1 m within hours (an equivalent of ∼10 days of base-inflow). The effect of this kind of breach resembles that described for the flood induced breaches above with a second phase of elevation of the bottom salinity as seawater enters the estuary through the breached sandbar.

The reduced salinity of the micro-estuary during the dry summer (**Figure 3b**) is incompatible with the typical summer high evaporation (Rimmer et al., 2009) and low precipitation rates (Goldreich, 2003). This discrepancy can only be explained by the higher frequency of sandbar breaches during winter that increased sea-river water exchange rate and exerted strong control on the estuary water salinity, water structure and, to some extent, dissolved oxygen level (**Figure 4**).

Summer anoxia is regularly attributed to elevated rate of bacterial activity during the season (Jonas, 1997; Borsuk et al., 2001). Our findings show that in micro-estuaries and probably other intermittently connected estuaries and lagoons (Borsuk et al., 2001) summer anoxia is exacerbated by the reduced rate of water exchange with the sea. For instance, during the summer of 2014 (**Figure 4D**) oxic conditions in the bottom water were only achieved because of seawater

entrance. While clearly a reduction of the organic and nutrients loads is the best solution for eutrophied estuaries, this is not always achievable. Increasing the water exchange rate with the sea can be achieved using relatively simple engineering means, while reduction of bacterial oxygen demand is much more complicated.

Sandbar breaches may have long- or short-term effects on bottom water oxygenation level in the estuary. The longevity of such changes depends on the duration and rate of water exchange with the sea and the ratio between oxygen uptake and physical and biological oxygen supply rate to the bottom water of the estuary. The lower the oxygen uptake compared to input, the longer the effect of a sandbar breach. The high BOD (**Supplementary Figure S5**), and the prevalence of anoxia and hypoxia at the bottom water of the Alexander estuary indicates a high oxygen uptake to input ratio (Suari et al., 2017).

Artificial breaches have been offered as a mechanism for enhancing the water quality in partially connected estuaries, but their effectiveness is controversial (Schallenberg et al., 2010). Since the small volume of micro-estuaries suggest that such intervention could potentially be more cost-effective than expensive improvements to wastewater treatment in the catchment, we examined the potential of sandbar breaches as a mitigation method to relieve oxygen stress. We analyzed breach events and an artificial breach of the sandbar. During the artificial breaching experiment, the sandbar at the estuary mouth was rebuilt by natural processes within hours and anoxia was reestablished 2 days after the breach. On the other hand, some of the prolonged flood breaches (type 1) were followed by long periods of oxygenated bottom water (**Figure 3b**). These observations suggest that while short term simple artificial interventions have a limited effect (days) on the hyper-eutrophic Alexander micro-estuary, the severity of anoxic conditions in micro-estuaries can be elevated by maintaining a sustained connection to the sea using proper engineering means.

The discrepancy between the fact that sandbar breaches are being used as a method for increasing bottom oxygen concentration in partially connected estuaries (Barton and Sherwood, 2004) and the fact that some scholars deem them ineffective (Becker et al., 2009) suggest the need for a method to evaluate and forecast the effectiveness of such breaches in maintaining oxygenated bottom water. This method should fit estuaries with varying eutrophication and respiration rates and different morphological characteristics. Such forecast could potentially be performed using numerical models. However, standard geophysical fluid dynamics models cannot simulate changes of bathymetry during model run. Therefore, for micro-estuaries such as the Alexander, where sandbar morphology dictates the state of the system to high degree, such models cannot achieve adequate forecast precision. To that end, we constructed a dilution-oxygenation diagram for the Alexander bottom water (**Figure 7** and **Supplementary Figure S6**) as a simple way to evaluate what is the minimum dilution with seawater that could supply enough oxygen to overcome the oxygen demand of the micro-estuary bottom water and sediment (**Figure 7**) and by that, achieve oxygenated bottom water. As evident from the large number of days (more than 70%) located below the zero day to day oxygen change in **Figure 7**, the bottom water is constantly losing oxygen throughout most of the days. When the bottom water are not being replenished with significant amount of new water (i.e., dilution with either fresh or salt water is lower than 10%), the estuary typically lost oxygen at an average rate of ~ -4.6 μmol L^{-1} day^{-1}, more than an order of magnitude lower than the BOD of these water ($\sim$80 μmol L^{-1} day^{-1}, **Supplementary Figure S5**). This difference may be partly attributed to diffusive mixing with oxygenated sea and surface water that compensate for some of the bottom oxygen uptake, but first and foremost, to the low oxygen concentration that characterizes the bottom water for prolonged periods of time (**Figures 3c**, **5a** and see also Suari et al., 2017). Note that anoxic water will not lose any more oxygen.

Sandbar breaches, evident by more than 5% dilution with seawater (**Figure 7**, right side) are the major renewal mechanism that replenishes the bottom water with new oxygen. Using the typical bottom salinity of 20 PSU (**Figure 3**) and seawater salinity of 39.5 PSU, we estimate that the required dilution rate of bottom water for sustainable oxygenation is in the order of 10% per day. Using **Figures 1**, **3**, we can estimate the bottom water volume to be a third of the estuary volume, $\sim 10^5$ m^3, therefore the required seawater flux is on the order of 10^4 m^3 d^{-1}, $\sim$60% of the median freshwater flux.

Climate change is expected to cause poleward movement of arid climate zones (Rubel and Kottek, 2010) which will cause expansion of arid region into more populated regions that are currently situated in temperate climate zones. This spread is expected to increase the demand for freshwater and increase the ratio of treated to natural water discharge into coastal stream and estuaries and hence to their eutrophication (Kennison and Fong, 2014). Evidence of this process is described by Ludwig et al. (2009). Another implication of climate change is a forecasted increase in the number of heavy precipitation events (Coumou and Rahmstorf, 2012) is likely to result in more frequent breaches of sandbars at the estuarine mouth (Vachtman et al., 2013).

CONCLUSION

- Micro-estuaries with their small water volume and <1 km^2 surface area are unique water bodies that show high temporal dynamics and are prone to anthropogenic impacts, but also amenable to small and cost-effective interventions.
- Analysis of natural and experimental sandbar breaches indicate that the current oxygen consumption rate of the Alexander micro-estuary is too high to consider sandbar breaches as a remedy for the bottom water anoxia. Nevertheless, it demonstrates the feasibility of small-scale interventions to control micro-estuary hydrology and biogeochemistry.
- A dilution oxygenation diagram (**Figure 7**) which only requires deployment and maintenance of two sensors (oxygen and salinity) can be a fast and handy tool to

determine the water exchange rate needed to reach oxic condition in partially connected estuary bottom water.

AUTHOR CONTRIBUTIONS

YS analyzed the data and wrote the manuscript. TA collected most of the data, analyzed the samples, and helped to write the manuscript. MG and TS helped for collecting the samples, and drafting and writing the manuscript. MK helped with writing the manuscript including correcting the English. SG is a Principal Investigator on the RIME project. TT assisted in field work and manuscript drafting, writing, and reviewing. GY headed the project and was part of drafting, writing, sampling, and data analysis.

FUNDING

This study was funded by an anonymous philanthropic fund, Ruppin Internal Grants numbers 34573 to YS and 3033 to GY, and Israeli Ministry of Science, Space, and Technology Grant number 12478-3 to GY.

ACKNOWLEDGMENTS

The authors would like to thank the staff of the School of Marine Sciences in Michmoret for their continuing support. A dedicated group of students who conducted the sandbar breach experiment: Maayan Neder, Meir Zur, Roni Zafriri, and Tom Reich. Reuben Rozenblat who constantly gets us out of trouble and Anat Tsemel for reviewing the manuscript.

SUPPLEMENTARY MATERIAL

The Supplementary Material for this article can be found online at: https://www.frontiersin.org/articles/10.3389/fmars.2019.00224/full#supplementary-material

REFERENCES

Avnaim-Katav, S., Agnon, A., Sivan, D., and Almogi-Labin, A. (2016). Calcareous assemblages of the southeastern Mediterranean low-tide estuaries - Seasonal dynamics and paleo-environmental implications. *J. Sea Res.* 108, 30–49. doi: 10.1016/j.seares.2015.12.002

Azov, Y. (1991). Eastern mediterranean—a marine desert. *Mar. Pollut. Bull.* 23, 225–232. doi: 10.1016/0025-326x(91)90679-m

Bárcena, J. F., Garcia, A., Gómez, A. G., Álvarez, C., Juanes, J. A., and Revilla, J. A. (2012). Spatial and temporal flushing time approach in estuaries influenced by river and tide. an application in Suances Estuary (Northern Spain). Estuar. *Coast. Shelf Sci.* 112, 40–51. doi: 10.1016/j.ecss.2011.08.013

Barrett, K. R. (2002). Estuary restoration and maintenance: the national estuary program. *Ecol. Eng.* 18:395. doi: 10.1371/journal.pone.0148220

Barton, A. J., and Sherwood, J. (2004). *PARKS VICTORIA TECHNICAL SERIES NUMBER 15 Estuary Opening Management in Western Victoria An Information Analysis*. Melbourne: Parks Victoria.

Baydoun, S., Ismail, H., Amacha, N., Arnold, N., Kamar, M., and Abou-Hamdan, H. (2016). Distribution pattern of aquatic macrophytic community and water quality indicators in upper and lower litani river Basins, Lebanon. *J. Appl. Life Sci. Int.* 6, 1–12. doi: 10.9734/JALSI/2016/25840

Becker, A., Laurenson, L. J. B., and Bishop, K. (2009). Artificial mouth opening fosters anoxic conditions that kill small estuarine fish. *Estuar. Coast. Shelf Sci.* 82, 566–572. doi: 10.1016/j.ecss.2009.02.016

Bianchi, C. N. (2007). Biodiversity issues for the forthcoming tropical mediterranean Sea. *Hydrobiologia* 580, 7–21. doi: 10.1007/978-1-4020-6156-1_1

Blaber, S. J. M., Cyrus, D. P., Albaret, J.-J., Ching, C. V., Day, J. W., Elliott, M., et al. (2000). Effects of fishing on the structure and functioning of estuarine and nearshore ecosystems. *ICES J. Mar. Sci.* 57, 590–602. doi: 10.1006/jmsc.2000.0723

Borsuk, M. E., Stow, C. A., Luettich, R. A., Paerl, H. W., and Pinckney, J. L. (2001). Modelling oxygen dynamics in an intermittently stratified estuary: estimation of process rates using field data. *Estuar. Coast. Shelf Sci.* 52, 33–49. doi: 10.1006/ecss.2000.0726

Boyes, S., and Elliott, M. (2006). Organic matter and nutrient inputs to the humber Estuary, England. *Mar. Pollut. Bull.* 53, 136–143. doi: 10.1016/j.marpolbul.2005.09.011

Burnison, B. K. (1980). Modified dimethyl sulfoxide (DMSO) extraction for chlorophyll analysis of phytoplankton. *Can. J. Fish. Aquat. Sci.* 37, 729–733. doi: 10.1139/f80-095

Celesri, L. S., Greenberg, A. E., and Eaton, A. D. (2012). *Standard Methods for the Examination of Water and Wastewater*. Washington, DC: American Public Health Association.

Coumou, D., and Rahmstorf, S. (2012). A decade of weather extremes. *Nat. Clim. Chang.* 2, 491–496. doi: 10.1038/nclimate1452

Day, J. W., Yanez-Arancibia, A., Kemp, W. M., and Crump, B. C. (2013). *Introduction to Estuarine Ecology*. Hoboken, NJ: Wiley-Blackwell.

Diaz, R. J., and Rosenberg, R. (2008). Spreading dead zones and consequences for marine ecosystems. *Science* 321, 926–929. doi: 10.1126/science.1156401

Ducrotoy, J.-P., and Elliott, M. (2006). Recent developments in estuarine ecology and management. *Mar. Pollut. Bull.* 53, 1–4. doi: 10.1016/j.marpolbul.2006.02.001

Elliott, M., and McLusky, D. S. (2002). The need for definitions in understanding estuaries. *Estuar. Coast. Shelf Sci.* 55, 815–827. doi: 10.1006/ecss.2002.1031

Everett, J. D. (2007). *Biogeochemical Dynamics of an Intermittently Open Estuary: a Field and Modelling Study*. Ph.D thesis, University of New South Wales, Sydney.

Gale, E., Pattiaratchi, C., and Ranasinghe, R. (2006). Vertical mixing processes in intermittently closed and Open Lakes and Lagoons, and the dissolved oxygen response. *Estuar. Coast. Shelf Sci.* 69, 205–216. doi: 10.1016/j.ecss.2006.04.013

Goldreich, Y. (2003). *The Climate of Israel: Observation, Research and Application*. New York, NY: Springer.

Grasshoff, K., Kremling, K., and Ehrhardt, M. (2009). *Methods of Seawater Analysis*. Hoboken, NJ: John Wiley & Sons.

Hastie, B. F., and Smith, S. D. A. (2006). Benthic macrofaunal communities in intermittent estuaries during a drought: comparisons with permanently open estuaries. *J. Exp. Mar. Bio. Ecol.* 330, 356–367. doi: 10.1016/j.jembe.2005.12.039

Hecht, A., Pinardi, N., and Robinson, A. R. (1988). Currents, water masses, eddies and jets in the Mediterranean Levantine Basin. *J. Phys. Oceanogr.* 18, 1320–1353. doi: 10.1175/1520-0485(1988)018%3C1320%3Acwmeaj%3E2.0.co%3B2

Herut, B., Kress, N., and Hornung, H. (2000). Nutrient pollution at the lower reaches of Mediterranean coastal rivers in Israel. *Water Sci. Technol.* 42, 147–152. doi: 10.2166/wst.2000.0306

Herut, B., Shefer, E., Rahav, E., Silverman, J., Gordon, N., Gertman, I., et al. (2015). *The National Monitoring Program of Israel's Mediterranean coastal waters – Scientific Report for 2013/14 - Climate change*. Haifa: IOLR.

Holmes, R. M., Aminot, A., Kérouel, R., Hooker, B. A., and Peterson, B. J. (1999). A simple and precise method for measuring ammonium in marine and freshwater ecosystems. *Can. J. Fish. Aquat. Sci.* 56, 1801–1808. doi: 10.1139/f99-128

Jonas, R. B. (1997). Bacteria, dissolved organics and oxygen consumption in salinity stratified chesapeake bay, an anoxia paradigm. *Integr. Comp. Biol.* 37, 612–620. doi: 10.1093/icb/37.6.612

Kennison, R. L., and Fong, P. (2014). Extreme eutrophication in shallow estuaries and lagoons of california is driven by a unique combination of local watershed modifications that trump variability associated with wet and dry seasons. *Estuar. Coasts* 37, 164–179. doi: 10.1007/s12237-013-9687-z

Kennison Krista Kamer, R., and Fong, P. (2003). *Nutrient Dynamics and Macroalgal Blooms: A Comparison of Five Southern California Estuaries*. Costa Mesa, CA: Southern California Coastal Water Research Project.

Krom, M. D., and Berner, R. A. (1981). The diagenesis of phosphorus in a nearshore marine sediment. *Geochim. Cosmochim. Acta* 45, 207–216. doi: 10.1016/0016-7037(81)90164-2

Krom, M. D., and Suari, Y. (2015). Eastern Mediterranean sea. a natural laboratory for studying marine biogeochemical processes. *Ocean Chall.* 21, 46–52.

Krom, M. D., Thingstad, T. F., Brenner, S., Carbo, P., Drakopoulos, P., Fileman, T. W., et al. (2005). Summary and overview of the CYCLOPS P addition lagrangian experiment in the Eastern Mediterranean. Deep. Res. Part II Top. *Stud. Oceanogr.* 52, 3090–3108. doi: 10.1016/j.dsr2.2005.08.018

Lichter, M., Zviely, D., and Klein, M. (2010). Morphological patterns of southeastern Mediterranean river mouths: the topographic setting of the beach as a forcing factor. *Geomorphology* 123, 1–12. doi: 10.1016/j.geomorph.2010.05.007

Ludwig, W., Dumont, E., Meybeck, M., and Heussner, S. (2009). River discharges of water and nutrients to the Mediterranean and Black Sea: major drivers for ecosystem changes during past and future decades? *Prog. Oceanogr.* 80, 199–217. doi: 10.1016/j.pocean.2009.02.001

Madden, C. J., Goodin, K., Allee, R. J., Cicchetti, G., Moses, C., Finkbeiner, M., et al. (2009). *Coastal and Marine Ecological Classification Standard*. Arlington, VA: NatureServe.

MathWorks Inc (2012). *Matlab*. Natick, MA: MathWorks Inc.

MathWorks Inc (2013). *MATLAB and Statistics Toolbox Release 2013b*. Natick, MA: The MathWorks, Inc.

Meeder, E., Mackey, K. R. M., Paytan, A., Shaked, Y., Iluz, D., Stambler, N., et al. (2012). Nitrite dynamics in the open ocean clues from seasonal and diurnal variations. *Mar. Ecol. Prog. Ser.* 453, 11–26. doi: 10.3354/meps09525

Merwade, V., Cook, A., and Coonrod, J. (2008). GIS techniques for creating river terrain models for hydrodynamic modeling and flood inundation mapping. *Environ. Model. Softw.* 23, 1300–1311. doi: 10.1016/j.envsoft.2008.03.005

Morris, A. W., and Riley, J. P. (1963). The determination of nitrate in sea water. *Anal. Chim. Acta* 29, 272–279. doi: 10.1016/s0003-2670(00)88614-6

Murphy, J., and Riley, J. P. (1962). A modified single solution method for the determination of phosphate in natural waters. *Anal. Chim. Acta* 27, 31–36. doi: 10.1016/S0003-2670(00)88444-5

OJEC (2000). *DIRECTIVE 2000/60/EC of the European Parliament and of the Council of 23 October 2000 Establishing a Framework for Community Action in the Field of Water Policy*. Brussels: Official Journal of the European Communities.

Ozer, T., Gertman, I., Kress, N., Silverman, J., and Herut, B. (2015). Interannual thermohaline (1979-2014) and nutrient (2002-2014) dynamics in the Levantine surface and intermediate water masses, SE Mediterranean Sea. *Glob. Planet. Change* 151, 1–8. doi: 10.1016/j.gloplacha.2016.04.001

Potter, I. C., Chuwen, B. M., Hoeksema, S. D., and Elliott, M. (2010). The concept of an estuary: a definition that incorporates systems which can become closed to the ocean and hypersaline. *Estuar. Coast. Shelf Sci.* 87, 497–500. doi: 10.1016/j.ecss.2010.01.021

Pye, K., and Blott, S. J. (2014). The geomorphology of UK estuaries: the role of geological controls, antecedent conditions and human activities. *Estuar. Coast. Shelf Sci.* 150, 196–214. doi: 10.1016/j.ecss.2014.05.014

QGIS Developement Team (2017). *QGIS Geographic Information System. Open Source Geospatial Foundation Project*. Available at: http://qgis.com doi: 10.1016/j.ecss.2014.05.014 (accessed December 5, 2017).

Rabalais, N. N., Diaz, R. J., Levin, L. A., Turner, R. E., Gilbert, D., and Zhang, J. (2010). Dynamics and distribution of natural and human-caused hypoxia. *Biogeosciences* 7:585. doi: 10.5194/bg-7-585-2010

Rabouille, C., Conley, D. J., Dai, M. H., Cai, W.-J., Chen, C. T. A., Lansard, B., et al. (2008). Comparison of hypoxia among four river-dominated ocean margins: the Changjiang (Yangtze), Mississippi, Pearl, and Rhone rivers. *Cont. Shelf Res.* 28, 1527–1537. doi: 10.1016/j.csr.2008.01.020

Rimmer, A., Samuels, R., and Lechinsky, Y. (2009). A comprehensive study across methods and time scales to estimate surface fluxes from Lake Kinneret. *Israel. J. Hydrol.* 379, 181–192. doi: 10.1016/j.jhydrol.2009.10.007

Rosen, D. S. (2000). "A review of sea level monitoring status in Israel," in *Intergovernmental Oceanographic Commission & International Commission for the Scientific Exploration of the Mediterranean Sea {MedGLOSS} Pilot Network Workshop and Coordination Meeting, Israel Oceanographic & Limnological Research*, Haifa, 15–17.

Rubel, F., and Kottek, M. (2010). Observed and projected climate shifts 1901-2100 depicted by world maps of the Köppen-Geiger climate classification. *Meteorol. Zeitschrift* 19, 135–141. doi: 10.1127/0941-2948/2010/0430

Saaroni, H., Halfon, N., Ziv, B., Alpert, P., and Kutiel, H. (2010). Links between the rainfall regime in Israel and location and intensity of Cyprus lows. *Int. J. Clim.* 30, 1014–1025. doi: 10.1002/joc.1912

Sanders, R. J., Jickells, T., Malcolm, S., Brown, J., Kirkwood, D., Reeve, A., et al. (1997). Nutrient fluxes through the Humber estuary. *J. Sea Res.* 37, 3–23. doi: 10.1016/S1385-1101(96)00002-0

Schallenberg, M., Larned, S. T., Hayward, S., and Arbuckle, C. (2010). Contrasting effects of managed opening regimes on water quality in two intermittently closed and open coastal lakes. *Estuar. Coast. Shelf Sci.* 86, 587–597. doi: 10.1016/j.ecss.2009.11.001

Schindler, D. W. (2012). The dilemma of controlling cultural eutrophication of lakes. *Proc. Biol. Sci.* 279, 4322–4333. doi: 10.1098/rspb.2012.1032

Schlitzer, R. (2018). *Ocean Data View.* .

Seitzinger, S. P., and Sanders, R. W. (1997). Contribution of dissolved organic nitrogen from rivers to estuarine eutrophication. *Mar. Ecol. Prog. Ser.* 159, 1–12. doi: 10.3354/meps159001

Shalem, Y., Weinstein, Y., Levi, E., Herut, B., Goldman, M., and Yechieli, Y. (2014). The extent of aquifer salinization next to an estuarine river: an example from the eastern Mediterranean. *Hydrogeol. J.* 23, 69–79. doi: 10.1007/s10040-014-1192-3

Sierra, J. P., Sánchez-Arcilla, A., González Del Río, J., Flos, J., Movellán, E., Mösso, C., et al. (2002). Spatial distribution of nutrients in the Ebro estuary and plume. *Cont. Shelf Res.* 22, 361–378. doi: 10.1016/S0278-4343(01)00061-9

Smith, V. H., Tilman, G. D., and Nekola, J. C. (1999). Eutrophication: impacts of excess nutrient inputs on freshwater, marine, and terrestrial ecosystems. *Environ. Pollut.* 100, 179–196. doi: 10.1016/S0269-7491(99)00091-3

Striem, H. L. (2015). Storm Surges and Unusual Sea Levels on Israel's Mediterranean Coast. *Int. Hydrogr. Rev.* 51.

Suari, Y., Shaish, L., Gafny, S., Amit, T., Gilboa, M., Brokovitch, E., et al. (2017). Prolonged Oxygen stress at Alexander estuary are caused by nutrient loads and changes in sea stream connectivity. *Ecol. Environ.* 3, 44–52.

Tagliapietra, D., Sigovini, M., and Ghirardini, A. V. (2009). A review of terms and definitions to categorise estuaries, lagoons and associated environments. *Mar. Freshw. Res.* 60, 497–509. doi: 10.1071/MF08088

Tal, A., Al Khateeb, N., Nagouker, N., Akerman, H., Diabat, M., Nassar, A., et al. (2010). Chemical and biological monitoring in ephemeral and intermittent streams: a study of two transboundary Palestinian–Israeli watersheds. *Intl. J. River Basin Manag.* 8, 185–205. doi: 10.1080/15715124.2010.491796

Tolkatchev, A. (1996). Global sea level observing system ({GLOSS}). *Mar. Geod.* 19, 21–62. doi: 10.1080/01490419609388069

Topaz, T., Egozi, R., Eshel, G., and Chefetz, B. (2018). Pesticide load dynamics during stormwater flow events in Mediterranean coastal streams: alexander stream case study. *Sci. Total Environ.* 625, 168–177. doi: 10.1016/j.scitotenv.2017.12.213

Vachtman, D., Sandler, A., Greenbaum, N., and Herut, B. (2013). Dynamics of suspended sediment delivery to the Eastern Mediterranean continental shelf. *Hydrol. Process.* 27, 1105–1116. doi: 10.1002/hyp.9265

Velasco, J., Lloret, J., Millan, A., Marin, A., Barahona, J., Abellan, P., et al. (2006). Nutrient and particulate inputs into the Mar Menor lagoon (Se Spain) from an intensive agricultural watershed. *Water Air Soil Pollut.* 176, 37–56. doi: 10.1007/s11270-006-2859-8

Zviely, D., Kit, E., and Klein, M. (2007). Longshore sand transport estimates along the Mediterranean coast of Israel in the Holocene. *Mar. Geol.* 238, 61–73. doi: 10.1016/j.margeo.2006.12.003

Conflict of Interest Statement: The authors declare that the research was conducted in the absence of any commercial or financial relationships that could be construed as a potential conflict of interest.